RSC Advances

PAPER

View Article Online
View Journal | View Issue

Cite this: *RSC Adv.*, 2017, **7**, 10463

Effects of preparation approaches on optical properties of self-assembled cellulose nanopapers

Weisheng Yang,[a] Liang Jiao,[a] Douyong Min,[b] Zhulan Liu[a] and Hongqi Dai*[a]

As a flexible, transparent and sustainable material, cellulose nanopapers will gradually replace traditional plastic materials in "green" electronics. However, it is tedious to prepare nanopapers, and the processes have significant effects on the properties of nanopapers. Herein, after TEMPO oxidation and high pressure homogenization, cellulose nanofibrils (CNFs) were successfully produced from the softwood fibers. Then, the nanopapers were fabricated from cellulose nanofibrils using casting and vacuum filtration, and their properties, such as surface morphology, internal structure and optical properties, were examined. The nanopapers produced by casting have much smoother surfaces than those of the nanopapers prepared by filtration. As a result of the varying degrees of light scattering on the surface, nanopapers prepared by filtration present relatively high optical haze (24.2%) and good transmittance (78%) at 550 nm wavelength, whereas nanopapers produced by casting show relatively low optical haze (2.9%) and excellent transmittance (88%). Therefore, the nanopapers prepared by casting and filtration present unprecedented applications in indoor and outdoor display devices, respectively.

Received 30th November 2016
Accepted 26th December 2016

DOI: 10.1039/c6ra27529j

rsc.li/rsc-advances

Introduction

As a sustainable and "green" material, cellulose has attracted abundant attention for its potential to replace non-renewable materials for applications in various traditional fields.[1,2] Treated by chemical and/or mechanical methods, cellulose nanofibrils (CNFs) can be extracted from natural cellulose.[3–5] CNFs exhibit numerous advantages such as a higher specific stiffness, aspect ratio, specific surface area, and transparency.[6–8] Recently, nanopapers consisting of CNFs, as a novel substrate to replace traditional glass and plastics in "green" electronics, have been studied in detail.[9] It was found that the optical properties of nanopapers have significant effects on their practical applications.[10] For example, nanopapers with a high haze have anti-glare properties, which are particularly important for outdoor displays[11] and solar cells.[12] However, nanopapers with a low haze and excellent transmittance can potentially be used for high definition displays.

Two approaches were used in this study for manufacturing nanopapers. One method is casting, where the CNFs aqueous solution is poured into a polystyrene Petri dish with a smooth bottom. When the water is evaporated, the CNF films are obtained.[13] However, this process is time-consuming, which typically takes several days or weeks.[14] Another method to prepare nanopapers is vacuum filtration, which is a procedure similar to papermaking. It consists of two steps including obtaining a gel layer by filtering the CNFs aqueous solution and forming a film by drying the gel layer.[15,16]

The microstructure of CNFs and nanopapers play significant roles in the performance of the nanopapers. For example, nanopapers with different thicknesses have different mechanical and thermomechanical properties.[17] A nanopaper designed with different diameter fibers and packing density presents different transmittance and optical haze.[18] Moreover, the procedures used to prepare CNF films significantly affect their mechanical properties.[19] The effects of different preparation procedures on the transparency, appearance, mechanical strength, vapor permeability, and shrinkage of the CNF films were comprehensively studied.[16,20,21] However, the influences of different production methods on surface morphology, internal structure, and optical properties of nanopapers have not been studied.

In this study, nanopapers were prepared using casting and vacuum filtration. All the nanopapers had a comparable thickness. The effects of different preparation methods on the surface morphology, internal structure, light transmittance and transmission haze were identified and compared. Furthermore, a mechanism of optical haze was illustrated. Compared to that of traditional papers, nanopapers display transparency because of the lower diameters of the fibers. Nanopapers produced by casting and filtration present different optical haze, which is a result of the varying degrees of light scattering on their surface.

[a]*College of Light Industry Science and Engineering, Nanjing Forestry University, Nanjing, 210037, China. E-mail: hgdhq@njfu.edu.cn; Tel: +86-25-85428932*
[b]*Guangxi University, Nanning, 530004, China*

Experimental

Materials

Commercially supplied, bleached softwood kraft pulp purchased from Suzano was used as the raw material. 2,2,6,6-Tetramethyl-1-piperidinyloxy (TEMPO) was purchased from Sigma-Aldrich. Sodium hypochlorite (NaClO), potassium bromide (KBr), sodium hydroxide (NaOH) and hydrochloric acid (HCl) were all laboratory grade (Aladdin reagent Co., Shanghai, China).

Preparation of CNFs

The softwood pulp with mechanical pretreatment (5 g) was suspended in deionized water at a concentration of 1 wt%. Then, TEMPO (0.08 g) and NaBr (0.8 g) were added into the solution and stirred at 500 rpm at room temperature for 4 h. The pH was adjusted to about 10.0 by HCl (20% v/v) and NaOH (0.5 mol L^{-1}). Then, the reaction was terminated by adding 10 mL of ethyl alcohol. The suspension was dialyzed using a regenerated cellulose membrane with 12 000–14 000 (D) after centrifuging at 3000 rpm three times. Eventually, the suspension was treated with a homogenizer (FB-110X, ShangHai LiTu Mechanical Equipment Engineering Co. Ltd., china) under a pressure of 550 bar for 40 min.

Fabrication of nanopapers

Casting was performed by pouring an aqueous 0.5% w/v CNF suspension into a polystyrene Petri dish with a smooth bottom and dried at 35 °C for a few days. The resulting nanopapers with thicknesses of 80–95 μm were placed at 23 °C and 50% RH for 24 h to balance the moisture.

Filtration was performed by filtering an aqueous 0.5% w/v CNF suspension through a filtering device (60 mm diameter). The filter membranes with 0.22 μm (PVDF) were supported to filter film in the filtering device. The wet nanopapers were stacked and placed between an assembly of filter membranes and dried at 98 °C and 0.9 MPa after placing them at room temperature for 10 h. The dried nanopapers with thicknesses of 80–95 μm were placed at 23 °C and 50% RH for 24 h to balance the moisture.

The details of the preparation processes are shown in Scheme 1.

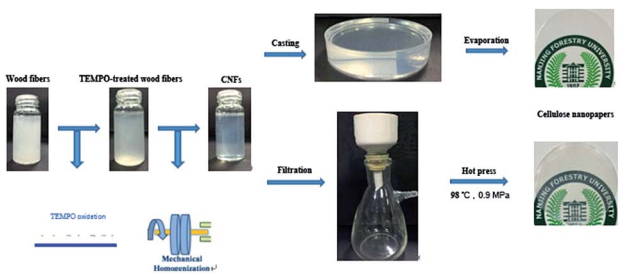

Scheme 1 The preparation processes of nanopapers.

Characterization

The carboxyl content of the CNFs was determined by the conductivity titration method.[22] The surface charge of the CNFs was characterized using a Zeta Potential Analyzer (Zetasizer Nano ZS, Malvern Instruments Ltd, UK) at room temperature. The crystalline structures of the natural cellulose and CNFs were determined using an X-ray diffractometer (Ultima IV, Rigaku, Japan) with Cu-Kα radiation ($\lambda = 15.4$). Scattered radiation was detected in the range of 5–40° at a scan speed of 4° min^{-1}. The thermal stability of natural cellulose and CNFs was measured using a thermogravimetric analyzer (TGA, Q5000IR, TA instruments, USA). About 5 mg of freeze-dried samples were weighed in a platinum pan and heated from 35 °C to 500 °C at a heating rate of 10 °C min^{-1} under high purity nitrogen with a flow rate of 40 mL min^{-1}. The dimensions of the CNFs were measured using atomic force microscopy operated in tapping mode (Dimension Edge, Bruker, Germany). For AFM analysis, a droplet of 0.001 wt% CNF aqueous solution was deposited on freshly cleaved mica, followed by drying. The surface morphology and the cross sections of the nanopapers were characterized using an environmental scanning electron microscope (Quanta-200, FEI, USA). By measuring the dimension and weight, the nanopapers' densities were calculated. The corresponding porosity for each sample was calculated as follows:

$$\text{porosity} = \left(1 - \frac{\rho_1}{\rho_2}\right) \times 100\% \quad (1)$$

where ρ_1 and ρ_2 are the densities of samples and cellulose, respectively ($\rho_2 = 1.5$ g cm^{-3}).

The surface morphology of the nanopapers was observed by AFM (Dimension Edge, Bruker, Germany) with a scan area of 8 × 8 μm^2. The optical haze and transmittance of samples were measured using a UV/VIS/NIR spectrophotometer (Lambda 950, PerkinElmer, USA) at a wavelength range of 200–1100 nm, according to the ASTM1003-13 standard method.[23]

Results and discussion

Properties of the CNFs

Wood fibers are the most abundant natural resources on earth and a sustainable and "green" material. Because of the carboxyl groups introduced into the surface of fibers, the bonding force between nanofibrils becomes weak, and with slight mechanical nanofibrillation, the TEMPO oxide fibers homogeneously disperse into CNFs.[24] With TEMPO/NaCl/NaBr oxidation and high-pressure homogenization, CNFs with a carboxylate content of 1.517 mmol g^{-1} were generated from natural fibers. From Fig. 1(a), atomic force microscopy (AFM) reveals that all of the CNFs had a diameter in the range of 20–25 nm. Compared with raw fibers, the aqueous 0.5% w/v CNF suspension exhibited excellent light transparency because the dimension of CNFs is much smaller than the wavelength of visible light (Fig. 1(b)). However, CNFs have high surface energy resulting in aggregation and flocculation.[25] These problems prevent its practical application. The existence of the carboxyl groups improved the

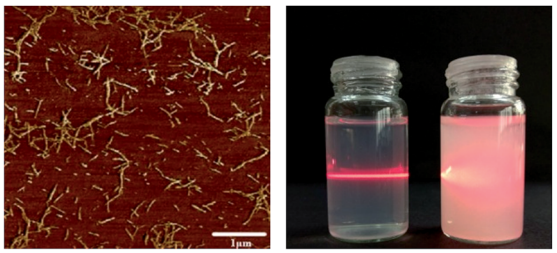

(a) (b)

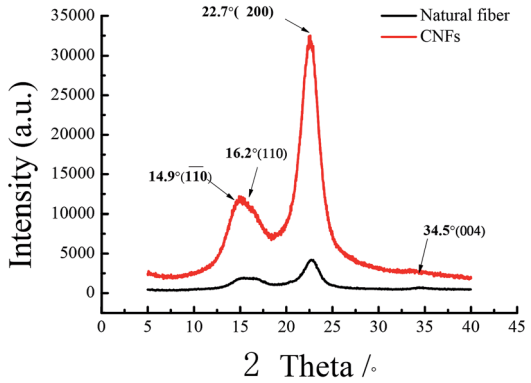

(c)

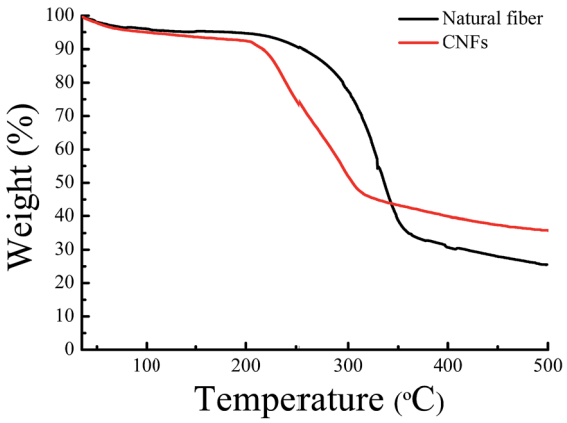

(d)

Fig. 1 (a) AFM morphology image of CNFs. (b) Photograph of CNFs and natural fibers in aqueous suspensions with 0.5% w/v. (c) X-ray diffraction spectra of CNFs and natural fibers. (d) TGA curves of CNFs and natural fibers.

water solubility of CNFs, and the CNFs could steadily disperse in an aqueous suspension through electrostatic repulsion. The zeta potential reflected the stability of the dispersion system.[26] The surface charge measurements indicated that the zeta potential value of the CNF aqueous solution (0.5% w/v) was −55 mV. The data showed that these CNFs had enough mutual electrostatic repulsion to steadily disperse in aqueous solution.

According to Fig. 1(c), all XRD profiles showed a typical cellulose I crystalline structure, with the diffraction peaks at 14.9°, 16.2°, 22.7° and 34.5° corresponding to 110, 110, 200 and 004 planes.[27] The data indicated that the TEMPO oxide treatment did not affect the crystalline structure of cellulose, which is in good agreement with Sun's result (2015).[28] While the amorphous region was removed during the chemical pretreatment, the CrI values increased from 71.4% to 76.9%. The TGA curves of the fibers and CNFs are shown in Fig. 1(d). In the low temperature region (<100 °C), all samples had a slight loss in quality, caused by the evaporation of absorbed water on the surface of the fibers. From 35 °C to 500 °C, the natural fibers and CNFs showed significant weightlessness. The fibers appeared remarkably weightless at 294 °C, and the residual carbon content was 25.5%. The CNFs had significant weightlessness at 214 °C, and the residual carbon was 35.4%, similar to results obtained by Lavoine (2016).[29] Due to the introduction of carboxyl groups on the surface of CNFs, the thermal stability appeared to show a steady and conspicuous decline from 294 °C to 214 °C.[16] The residual carbon content of CNFs was more than that of natural fibers, which was attributed to the breaking of the lignin and hemicelluloses. As the CNFs were extracted from natural fibers, the thermal stability of cellulose clearly appeared to decline. However, it was still higher than that of most of the flexible transparent plastic substrates, such as polyethylene terephthalate (PET), polyethylene naphthalate (PEN) and polycarbonate (PC).[30]

Morphology of nanopapers

Using the traditional papermaking method, regular papers consisting of wood fibers with a diameter approximately 25 μm were produced. The surface morphology of regular papers and nanopapers is shown in Fig. 2(a)–(c). Masses of micro-sized pores and a loose network structure were observed using SEM. During the decrease in the dimension of fibers, the nanoscale CNFs closely intertwined, and compact structures were obtained. The nanopapers produced by casting have a smoother and flatter surface compared to that of the nanopapers produced by filtration. Similar results were obtained by Sehaqui (2010).[14] The nanopapers have nanoscale surface roughness, which make them suitable to assemble transparent optical electronic devices, such as display devices and solar cells.[31,32] In fact, the production processes have a significant influence on surface roughness. Fig. 2(d)–(g) show the AFM height maps and 3D images of the surface of the nanopapers with a scan area of 8 × 8 μm^2. The nanopapers that were prepared by casting showed a much smoother morphology than that of the nanopapers prepared by filtration. According to the 3D images, it was found that the peak-to-valley height of nanopapers prepared by filtration was 32.6 nm, while for those produced by casting was only 12.2 nm. The AFM height maps revealed that the nanopapers prepared by filtration had a rough surface with 46.3 nm for the root-mean-square roughness. Compared with filtration, nanopapers produced by casting had a smoother surface with 3.3 nm for the root-mean-square roughness. It is the result of the separating procedure of the

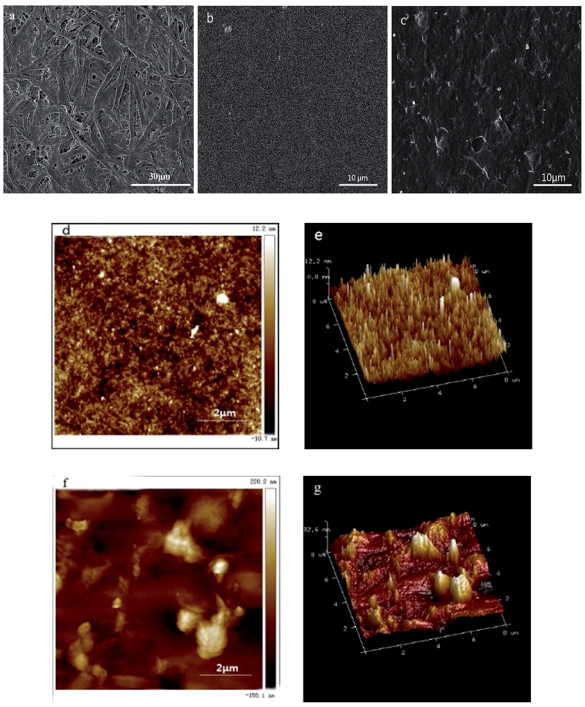

Fig. 2 (a–c) SEM images of the surface of the regular papers and the nanopapers prepared by casting and filtration. (d and e) AFM height images and 3D AFM images (scan area, 8 × 8 μm^2) of the nanopapers produced with casting. (f and g) AFM height images and 3D AFM images (scan area, 8 × 8 μm^2) of the nanopapers prepared by filtration.

nanopapers from the membranes in the process of filtration. In the process of filtration, being peeled from filter membrane made the surface of nanopapers become more rougher.[33] After evaporating the moisture of casting completely, nanopapers could be easily separated from the polystyrene Petri dish. Moreover, the Petri dish had a smooth face, which induced a smoother surface.

Internal structures of nanopapers

The cross-sectional structures of the nanopapers are shown in Fig. 3(b) and (c). Because of the same amounts of CNF suspensions, the thicknesses of the nanopapers that resulted from casting were similar to those obtained by filtration, which ranged from 80–95 μm in the SEM images. As the CNFs tightly intertwined with each other, the nanopapers exhibited smooth blade-cut cross sections. Its layered structure could not be clearly observed, which was different from the loose structure of the regular papers in Fig. 3(a). In addition, the moisture content, density and porosity of these nanopapers are shown in Table 1. The regular papers had lower densities and higher porosity values than those of the nanopapers, which were consistent with the SEM images. Moreover, the preparation approaches have limited effects on the nanopapers internal structures and moisture content. Previous studies (Qing 2015) found similar results.[19]

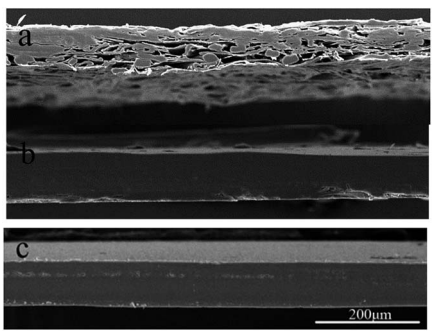

Fig. 3 (a–c) SEM images of the cross-sectional structures.

Optical properties of nanopapers

The light transparency and transmission haze can be tailored by changing the dimension and packing density of fibers.[34] Regular papers made from conventional cellulose fibers (~25 μm) have a loose internal structure. Because the fibers' dimension is much larger than visible wavelength, the light seriously scatters off the normal direction. There are also several micropores within the regular papers. The differences between the refraction indexes of air (1.0) and cellulose (1.5) increase the light scattering and reduce the transparency of the regular papers. According to Fig. 5, regular papers had limited light transmittance, which is only 0.1% at 550 nm. Due to the extremely fine nanofibril dimension, the nanopapers consisting of CNFs had great light transmittance. Although having similar packing density, the nanopapers prepared by casting and filtration showed different optical properties. From the transmittance curve in Fig. 5(g), the nanopapers with a smooth surface produced by casting showed the greatest transparency, followed by the PET films, which were taken as a reference, and then the nanopapers with a rough surface prepared by filtration. The transmittance was 88% for casting, 83% for PET films, and

Table 1 Density and porosity of nanopapers

Samples	Density (g cm^{-3})	Porosity (%)	Moisture content (%)
Casting	1.252	16.6	10.2
Filtration	1.248	16.8	8.2
Regular papers	0.616	58.9	—

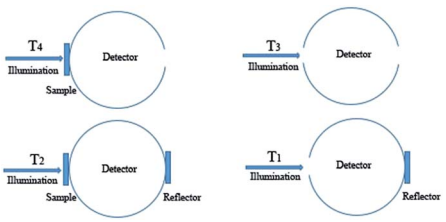

Fig. 4 The experimental haze measurement set up: T4 total forward scattered illumination; T3 total transmitted illumination; T2 and T1 are the corrections for the experimental setup.[36]

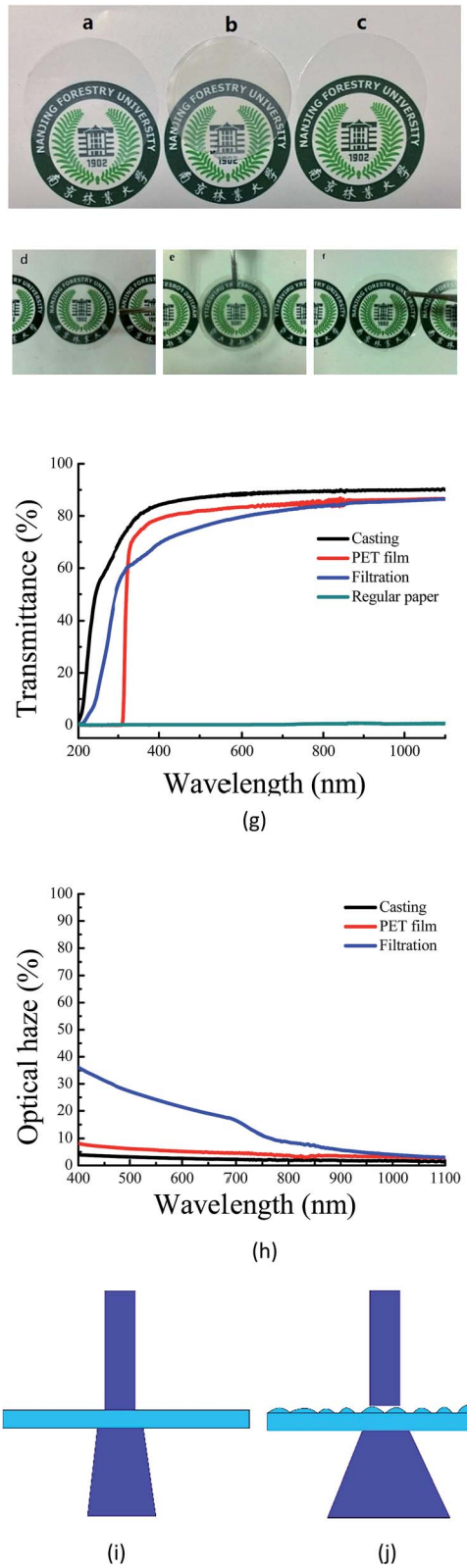

Fig. 5 (a–c) Digital photographs of the PET, the nanopapers prepared by casting and filtration. (d–f) Digital photographs of the PET, the nanopapers prepared by casting and filtration at a distance from the pattern underneath. (g) Light transmittance spectra of the PET, the nanopapers prepared by casting and filtration. (h) The haze value of the PET, the nanopapers prepared by casting and filtration. (i and j) the mechanism of light scattering of the nanopapers prepared by casting and filtration with optical difference.

78% for filtration at 550 nm.[35] In order to demonstrate the differences of all of these samples, they were placed on patterned paper (Fig. 5). The images under the PET film and nanopapers produced by casting were much clearer than those of the nanopapers prepared by filtration.

As an important optical property of the transparent electronic devices, optical haze can be described as the light scattering proportion of the total transmittance. It is experimentally described as follows:

$$\mathrm{HAZE} = \left[\frac{T_4}{T_2} - \frac{T_3}{T_1}\right] \times 100\% \quad (2)$$

where T_1, T_2, T_3, and T_4 are defined in Fig. 4.

As shown in Fig. 5(h), the PET film and nanopapers produced by casting had low transmission haze of 5.4% and 2.9% at 550 nm, respectively. The nanopapers prepared by filtration had a high optical haze of 24.2%. If the PET film and nanopapers were lifted with a certain height from the patterned paper, the pattern could be observed clearly through both the PET film and nanopapers produced by casting (Fig. 5(d)–(f)); however, the pattern under the nanopapers prepared by filtration appeared unclear. The nanopapers with different optical haze can be applied in numerous different fields.[12] The nanopapers prepared by filtration have relatively good light transmittance of 78% and a high optical haze of 24.2% at 550 nm. Due to the high transmission haze, it can be applied in outdoor displays. The nanopapers produced by casting have an excellent light transmittance of 88% at 550 nm and low optical haze of 2.9% at 550 nm. It is suitable for indoor high-definition display devices. The results of the optical haze are similar to those reported by Zhu (2015).[10] By decreasing the size and improving the packing density of CNFs, the transmission haze could be extremely decreased.[31]

In this study, nanopapers prepared by casting and filtration using 20–25 nm of CNFs have a similar packing density and porosity. The surface morphology shows that two types of nanopapers have different surface roughness, which leads to the alternations in surface light scattering. According to the schematic maps (Fig. 5(i) and (j)), the nanopapers prepared by filtration have a rough surface with 46.3 nm of root-mean-square roughness, which induces serious light scattering. Through nanopapers with a 24.2% transmission haze, the transmitted light deviated the in the incident direction. Unlike those with filtration, the nanopapers produced by casting show a smooth surface with 3.3 nm of root-mean-square roughness and 2.9% optical haze, and therefore there is negligible light scattering. Moreover, its transmitted light is mainly concentrated in the incident direction.

Conclusion

After TEMPO oxidation and high pressure homogenization, cellulose nanofibrils (CNFs) were successfully generated from softwood fibers. Then, nanopapers were prepared by casting and vacuum filtration, which exhibited significant differences in surface morphology, roughness, and optical properties. Although numerous diversities exist, the abovementioned two

types of nanopapers have a similar internal structure and excellent transparency. The relation between the surface roughness and optical haze was computationally studied. Because of strong light scattering, the rough surface generates a higher optical haze than that of the smooth surface. Nanopapers produced by casting have a smooth surface, excellent light transmittance, and low transmission haze. As a type of high-definition thin membrane material, these nanopapers can be applied into HD displays. In contrast, nanopapers prepared by filtration showed a relatively rough surface, good light transmittance, and high optical haze. In addition, because of the high optical haze, the nanopapers have anti-glare functionality, with potential uses in indoor display devices.

Acknowledgements

This study was conducted with Yang who was a PhD student at Nanjing Forestry University, Nanjing, China. This study was partially supported by the State Forestry Administration of China (Project No. 2015-4-54) and the National Natural Science Foundation of China (Project No. 31470599). This study was also supported by the Priority Academic Program Development of Jiangsu Higher Education Institutions (PAPD) in China.

References

1 R. J. Moon, A. Martini, J. Nairn, J. Simonsen and J. Youngblood, *Chem. Soc. Rev.*, 2011, **40**, 3941–3994.
2 S. J. Eichhorn, *Soft Matter*, 2010, **7**, 303–315.
3 J. H. Kim, B. S. Shim, H. S. Kim, Y. J. Lee, S. K. Min and D. Jang, *International Journal of Precision Engineering and Manufacturing-Green Technology*, 2015, **2**, 197–213.
4 T. Zimmermann, E. Pöhler and T. Geiger, *Adv. Eng. Mater.*, 2004, **6**, 754–761.
5 T. Saito, S. Kimura, Y. Nishiyama and A. Isogai, *Biomacromolecules*, 2007, **8**, 2485–2491.
6 Z. Yin and Q. Zheng, *Adv. Eng. Mater.*, 2012, **2**, 179–218.
7 M. Nogi and H. Yano, *Adv. Mater.*, 2008, **20**, 1849–1852.
8 P. Terech, L. Chazeau and J. Y. Cavaille, *Macromolecules*, 1999, **32**, 1872–1875.
9 M. Irimia-Vladu, *Chem. Soc. Rev.*, 2013, **43**, 588–610.
10 H. L. Zhu, Z. Q. Fang, W. Zhu, J. Dai, Y. Yao and S. Fei, *ACS Nano.*, 2015, **10**, 1369–1377.
11 B. T. Liu, Y. T. Teng, R. H. Lee, W. C. Liaw and C. H. Hsieh, *Colloids Surf., A*, 2011, **389**, 138–143.
12 Z. Q. Fang, H. L. Zhu, Y. Yuan, D. Ha, S. Zhu and C. Preston, *Nano Lett.*, 2014, **14**, 765–773.
13 C. Aulin, M. Gallstedt and T. Lindstrom, *Cellulose*, 2010, **17**, 559–574.
14 H. Sehaqui, A. Liu, Q. Zhou and L. A. Berglund, *Biomacromolecules*, 2010, **11**, 2195–2198.
15 M. Henriksson, L. A. Berglund, P. Isaksson, T. Lindström and T. Nishino, *Biomacromolecules*, 2008, **9**, 1579–1585.
16 H. Fukuzumi, T. Saito and T. Iwata, *Biomacromolecules*, 2009, **10**, 162–165.
17 Q. Li, W. Chen, Y. Li, X. Guo, S. Song and Q. Wang, *Cellulose*, 2016, **23**, 1375–1382.
18 H. L. Zhu, Z. Q. Fang, C. Preston, Y. Li and L. B. Hu, *Energy Environ. Sci.*, 2013, **7**, 269–287.
19 Y. Qing, R. Sabo, Y. Wu, J. Y. Zhu and Z. Cai, *Cellulose.*, 2015, **22**, 1091–1102.
20 A. Retegi, N. Gabilondo and C. Pena, *Cellulose*, 2009, **17**, 661–669.
21 M. Henriksson and L. A. Berglund, *J. Appl. Polym. Sci.*, 2007, **106**, 2817–2824.
22 A. D. French, *Cellulose*, 2014, **21**, 885–896.
23 ASTM D1003-13, *Standard Test Method for Haze and Luminous Transmittance of Transparent Plastics*, ASTM International, West Conshohocken, PA, 2013, https://www.astm.org.
24 T. Saito, Y. Nishiyama, J. L. Putaux, M. Vignon and A. Isogai, *Biomacromolecules*, 2006, **7**, 1687–1691.
25 O. Nechyporchuk, M. N. Belgacem and J. Bras, *Ind. Crops Prod.*, 2016, **93**, 2–25.
26 F. Azzam, L. Heux and J. Putaux, *Biomacromolecules*, 2010, **11**, 3652–3659.
27 G. H. Tonoli, E. M. Teixeira, A. C. Correa, J. M. Marconcini, L. A. Caixeta, M. A. Pereiradasilva and L. H. Mattoso, *Carbohydr. Polym.*, 2012, **89**, 80–88.
28 X. Sun, *Cellulose*, 2015, **22**, 1123–1133.
29 N. Lavoine, J. Bras and T. Saito, *Macromol. Rapid Commun.*, 2016, **37**, 1033–1039.
30 S. M. Priv Doz, *Angew. Chem., Int. Ed.*, 2004, **43**, 1078–1085.
31 J. Huang, H. Zhu, Y. Chen, C. Preston, K. Rohrbach, J. Cumings and L. Hu, *ACS Nano*, 2013, **7**, 2106–2113.
32 H. L. Zhu, Z. Xiao, D. Liu, Y. Li, N. J. Weadock, Z. Fang, J. Huang and L. Hu, *Energy Environ. Sci.*, 2013, **6**, 2105–2111.
33 T. Tammelin, U. Hippi and A. Salminen, EP, EP2771390[P], 2014.
34 H. L. Zhu, S. Parvinian, C. Preston, O. Vaaland, Z. Ruan and L. B. Hu, *Nanoscale*, 2013, **5**, 3787–3792.
35 M. Nogi, S. Iwamoto, A. N. Nakagaito and H. Yano, *Adv. Mater.*, 2009, **21**, 1595–1598.
36 C. Preston, Y. Xu, X. Han, J. N. Munday and L. B. Hu, *Nano. Res.*, 2013, **6**, 461–468.

